Diffraction study of solid oxygen embedded in porous glasses

D. Wallacher,[1] R. Ackermann,[1] P. Huber,[1,2] M. Enderle,[1,3] and K. Knorr[1]
[1]*Technische Physik, Universität des Saarlandes, D 66041 Saarbrücken, Germany*
[2]*Department of Physics, Harvard University, Cambridge, Massachusetts 02138*
[3]*Institut Laue-Langevin, BP156, F-38042 Grenoble, France*
(Received 8 May 2001; published 24 October 2001)

Molecular oxygen condensed and solidified in porous silica with pore diameters of 5, 7.5, and 13 nm has been investigated by x-ray diffraction as function of the filling fraction and the temperature. Two components of the pore filling can be distinguished: an amorphous layer on the pore walls, about 2 ML thick, with no conspicuous temperature dependence and the capillary condensate in the pore center that shows the sequence liquid-γ-β of bulk O_2, but with reduced transition temperatures. In 5-nm pores the γ-β transformation is incomplete. In the larger pores remainders of the β-α transition have been detected.

DOI: 10.1103/PhysRevB.64.184203 PACS number(s): 61.10.Nz, 61.43.Gt, 64.70.Nd

I. INTRODUCTION

It is well established that the freezing and melting points of a vast variety of materials, ranging from cryoliquids to water and metals, embedded in narrow pores are reduced and that there is considerable thermal hysteresis between freezing and melting.[1–7] For Vycor glass, a prominent porous matrix with a pore diameter of a few nanometer, the reduction is typically of the order of 10%.

Of course, the question arises whether analogous effects occur for solid-solid transitions. There are in fact some few examples of structural studies on solidified pore fillings. Ice, an obvious candidate for polymorphic transitions, crystallizes in pores in the cubic (I_c) rather than in the ordinary hexagonal (I_h) modification and there is no evidence for a crystallographic phase transition.[5] Solid N_2 in nanometer pores remains in the high-T β structure down to the lowest temperatures.[8,9] The β-α structural phase transition occurring in the bulk system is obviously suppressed. However, in pore-condensed CO, which in the bulk state is isomorphous to N_2, the β-α transition still occurs. On cooling the β-α transition of CO is shifted to lower T, similar to the melting transition. On warming an intermediate orientationally disordered fcc phase appears, which is unknown in the bulk state.[9] For previous results on O_2, see below.

The phase sequence of bulk O_2 is liquid-γ-β-α with the melting point at 54.4 K and the γ-β and β-α solid-solid (first-order) transitions at 44 K and 23.9 K. The γ phase is cubic Pm3n, paramagnetic and orientationally disordered with two inequivalent sites with spherelike and disklike orientational distributions of the molecular axis. In the rhombohedral $R\bar{3}m$ β phase the molecular axes are all parallel, along the threefold crystallographic axis. The spins lie in the basal plane and form a short-range-ordered version of a 120-deg Néel state. The low-T monoclinic α phase is a simple collinear antiferromagnet. The chemical lattice of the α phase is derived from the β phase through a homogeneous distortion of magnetoelastic origin. O_2 thus combines structural and magnetic aspects.[10–12] It is presumably for this reason that there is considerably more information on O_2 than on most other smaller molecules embedded in pores: The early magnetic studies of Gregory[13,14] concentrate on relatively low fractional pore fillings that he regards as an example of an amorphous antiferromagnet. The optical study of Awschalom and Warnock[2] has established the dependence of the melting and freezing temperatures as well as of a solid-solid transformation temperature (which they interpret as the γ-β transition) on the pore diameter. These authors are also among the first who distinguish between an adsorbate on the pore walls and the capillary condensate in the pore center. Molz *et al.*[3] report heat-capacity measurements on the liquid-solid and the solid-solid transition. Both transitions were found to be hysteretic and similarly shaped anomalies. Schirato *et al.*[15] performed neutron-diffraction measurements on different pore sizes. In 6-nm pores, the solid is found to form structures that are consistent with those of the γ and β bulk phases. For narrower pores, however, the authors propose an amorphous structure that they call less ordered than the liquid phase. In all these studies various types of porous silica have been used as substrate.

This paper presents a systematic x-ray-diffraction study on O_2 in silica samples with three different pore sizes as function of temperature and filling.

II. EXPERIMENTAL

The porous substrates of our study are a Vycor glass (Corning) that turned out to have an average pore diameter D of 13 nm (see below) and two xerogels (''GELSIL,'' Geltech Inc. Orlando, FL) with D values of 7.5 nm and 5 nm, as specified by the supplier. Both types of porous glass are practically pure SiO_2 and there are no indications in our work that the pores are in any way different except for the diameter and a slightly larger porosity of the xerogels. For further information on the porous substrates, see the electron-microscope studies and the small-angle x-ray and neutron studies of Refs. 16–18. Our own small-angle x-ray results indicate that the pores are randomly oriented in space.

The samples have been filled with oxygen well above the bulk melting point by adsorption out of the vapor phase (rather than by letting the liquid to be soaked in). The vapor-pressure isotherms, that is, the quantity n of O_2 adsorbed in the pores vs the vapor pressure P are shown are in Fig. 1

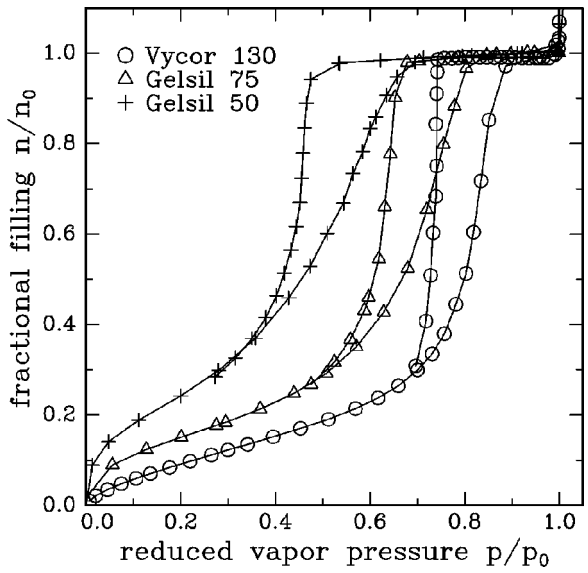

FIG. 1. Adsorption isotherms of O_2 for the three porous silica substrates used in this study. $T=85$ K for the 7.5-nm xerogel and $T=70$ K for 5-nm xerogel and the 13-nm Vycor glass. The quantity adsorbed is normalized to the complete filling, the vapor pressure to its saturated value.

using reduced units, $p=P/P_0$, $f=n/n_0$. Here P_0 is the saturated vapor pressure and n_0 the complete filling. The f values actually investigated by x-ray diffraction are 0.89, 0.41, 0.36, and 0.27 for the 7.5-nm xerogel, 0.90, 0.44, 0.34, 0.27, and 0.14 for the 5-nm xerogel, whereas the Vycor sample has been studied with an almost-complete filling of 0.95, only.

The pore diameter D can be determined from the f-p isotherm in two ways. The initial part of the isotherm is due to the growth of an adsorbed layer on the pore walls. Here the isotherm is well described by the Brunauer, Emmett, and Teller (BET) model.[19] A fit of this model to the data yields the active surface. Combining this information with the porosity, the pore diameter can be calculated assuming homogeneous cylindrical pores. The hysteretic part of the isotherm at higher f, $f>f_c$ is due to capillary condensation.[20] The vapor pressure at which the pores empty on desorption is related to the radius of curvature of the meniscus of the capillary condensate and to the surface tension via the Kelvin equation. It is usually assumed that this radius is equal to the pore radius. Clearly, both ways of extracting the pore diameter are standard, but require the knowledge of crucial parameters (namely, the area per molecule for the first method and the surface tension for the second method) and rely on some questionable assumptions. We quote D values based on the Kelvin equation. For the two xerogels we arrived at the D values specified by the supplier. The BET-based values are larger by about 20%.

The x-ray-diffraction setup consists of a conventional two-circle diffractometer with monochromatized Cu K_α radiation emanating from a rotating anode running at 10 kW. Coupled 2θ-θ scans of the Bragg-Brentano scattering geometry have been used. A typical counting time is 30 s per step. For the 2θ resolution of the instrument, see Fig. 2.

The distribution of diffracted intensity in reciprocal space

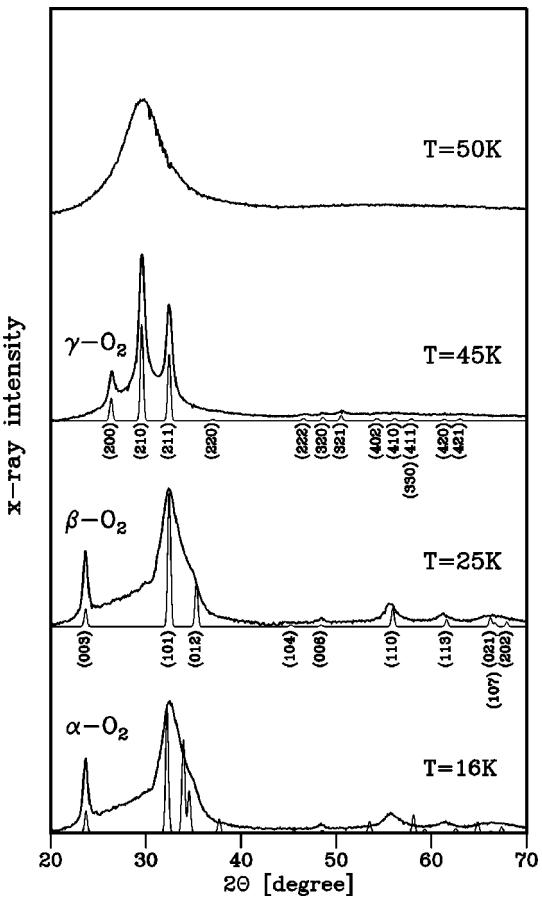

FIG. 2. Diffraction patterns of a complete filling of O_2 in 7.5-nm pores at selected temperatures. The background intensity of the empty substrate has been subtracted. Also shown are patterns of the three crystalline phases α, β, γ of bulk O_2 as calculated on the basis of Ref. 11. The width of the calculated powder lines gives the resolution of the diffractometer.

has also been investigated by different types of scans, for which the scattering vector is no longer perpendicular to the surface of the samples, rocking scans in particular. It turns out that the samples do not show any texture that they are isotropic powders in the sense of powder diffractometry.

The samples are mounted inside an all-metal cell having the shape of an equilateral triangular prism. Two of the faces are equipped with Be windows for the passage of the incoming and the outgoing x-ray beam.

Cooling down a porous sample filled with a condensed gas is a problem. There is a temperature interval in which the vapor pressure is of the order of 10^{-4} to 10^{-7} Torr, which is already too low in order to guarantee a good thermal contact between the glass sample and the cell walls via the vapor, but still large enough for the distillation of the condensate out of the pores onto the colder walls to occur on the time scale of the experiment. This loss may be reduced, but not completely suppressed by a carefully chosen cooling rate and a good mechanical contact between the glass sample and the cell, but eventually we only managed to keep the material in the pores by adding some millibars of He contact gas when working at temperatures below 55 K.

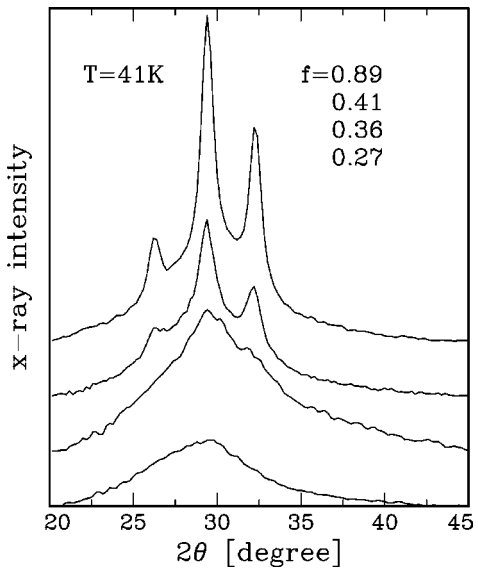

FIG. 3. Diffraction patterns for four different fillings of 7.5 nm pores at 41 K. The background intensity of the substrate has been subtracted.

III. RESULTS AND DISCUSSION

A. Structures

For all three pore sizes the diffraction patterns are liquidlike at higher temperatures, but show Bragg peaks at low temperatures. See Fig. 2 for an overview on O_2 in the 7.5-nm xerogel. The pattern recorded at 50 K, a temperature well below the bulk triple point, suggests that the pore filling is still liquid at this temperature. The broad peak around $2\theta = 30$ deg is interpreted as the first maximum of the structure factor of the liquid. The maximum shifts to larger angles on cooling. Within the experimental error this shift is consistent with the thermal expansion coefficient of the bulk liquid (extrapolated to temperatures below the bulk melting point). The width of the peak narrows on cooling, by about 10% between 60 K and 50 K, suggesting an increase of the correlation length of the liquid.

At lower T the patterns show relatively well-defined Bragg peaks. Here the pore condensate or at least a part of it is obviously crystalline. As already mentioned above and discussed in detail in our previous work on Ar (Refs. 7 and 21) one can distinguish two components of pore solid, an amorphous coating of the pore walls (for $f<f_c$) and a capillary condensed solid in the pore center (for $f>f_c$). The Bragg peaks of the solid state stem from the capillary condensate. As can be seen from the isotherms of Fig. 1 the f_c value (of the liquid regime) is about 0.35 for the 7.5-nm and 0.4 for 5-nm pores, what in both cases corresponds to a limiting thickness of the adsorbate layer of roughly three monolayer equivalents. In the solid regime, f_c can be estimated from the evolution of the diffraction pattern with f. See Fig. 3 for the 7.5 nm pores at 41 K: For $f=0.27$ the pattern is that of the amorphous wall coating. For $f=0.36$ first indications of sharper features superimposed on the amorphous background appear, which for $f=0.41$ have developed into Bragg peaks.

The Bragg peaks of the three solid phases of bulk O_2 at ambient pressure as calculated from the structural data of Krupskii *et al.*[11] and of Barrett *et al.*[12] are included in Fig. 2. The Miller indices of the Bragg peaks of the β phase refer to the hexagonal setting. The width of the peaks of the calculated patterns reflects the 2θ resolution of our experiment. The comparison of the experiment and the calculation shows that the pore solid is in the γ phase at 45 K and in the β phase at 25 K. Not only the strong reflections expected for the two phases at low scattering angles could be detected but several weaker ones at higher angles 2θ, such as $(320)_\gamma$ or $(113)_\beta$ can also be observed. Thus the pore solid, or more exactly its capillary condensed component, reproduces the phase sequence of bulk O_2 at ambient pressure liquid-γ-β but with lowered transition temperatures, considerable thermal hysteresis and wide-coexistence regions, as will be discussed below.

Does the capillary condensate eventually transform into the low-T α phase? In an x-ray diffraction experiment the β-α transition of bulk O_2 shows up via a splitting of some powder lines, in particular of the $(110)_\beta$ line. See the calculated patterns of α and β bulk O_2 in Figs. 2 and 4. The experiment fails to give clear-cut evidence for such a splitting, but at 16 K, the lowest temperature of our setup, the $(110)_\beta$ line is somewhat broadened in the 7.5-nm pores and slightly split in the 13-nm pores (Fig. 4). The T dependence actually suggests that these subtle changes of the peak profiles have almost saturated at 16 K such that we do not expect much more of a change below 16 K. A magnetic study of O_2 in the same samples has produced convincing evidence for the β-α transition to occur at about 20 K in the 13-nm pores and at about 18 K in the 7.5-nm pores.[22] Combining the magnetic and the structural information we propose that a β-α-like antiferromagnetic ordering of the spins still takes place in pores of this size, but the accompanying homogeneous magnetoelastic distortion of the lattice is reduced and replaced by more local strains.

The width of the powder lines exceeds the instrumental resolution by far. For the γ phase the intrinsic width is independent of $\sin\theta$ within the experimental error. This suggests the finite size L of the crystallites rather than inhomogeneous lattice strains to be the dominant reason for the line broadening. The values derived for L are given in Table I. For all three substrates studied, L is close to, in fact somewhat larger than, the pore diameter D even though the difference of L and D is of the order of the experimental error. The free diameter available for the capillary condensate is actually lower than the nominal pore diameter D by about 1 nm, because of the amorphous layer on the walls. Thus we propose that the γ crystallites are coherent across the free pore diameter but are somewhat larger along the pore axis, such that the resulting isotropic average L settles at a value slightly larger than D.

Schirato *et al.* have observed relatively sharp Bragg peaks the width of which translates into a value of L between 60 and 100 nm, an order of magnitude larger than the pore diameter of 6 nm. Sharp Bragg peaks can, of course, be due to bulk material outside the pores. We recall our discussion of the problems when cooling down pore fillings.

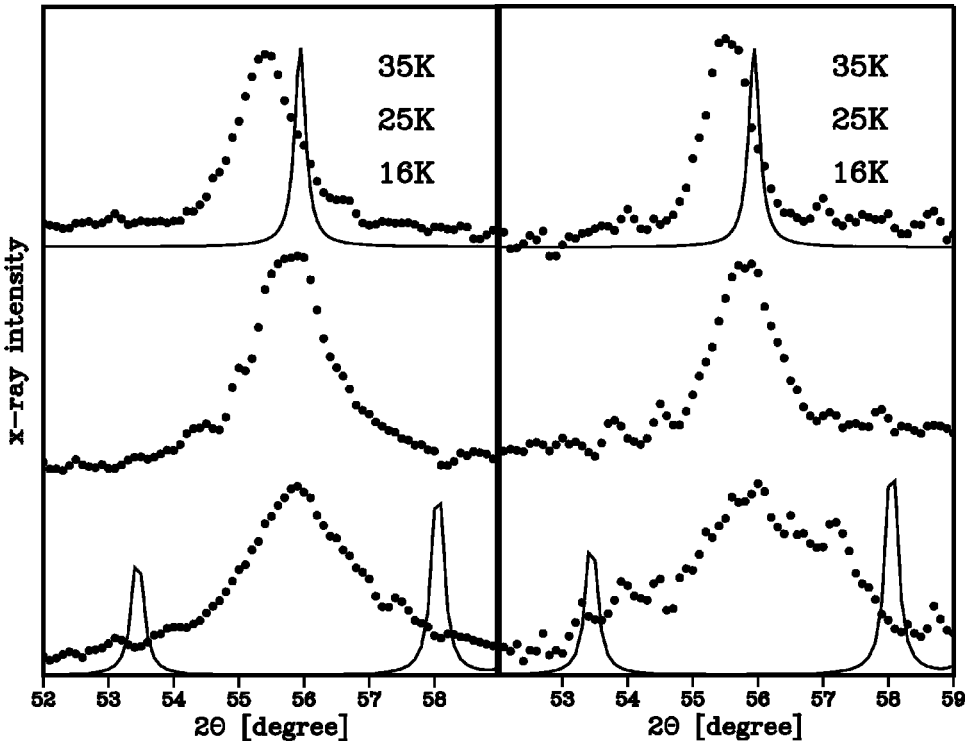

FIG. 4. The variation of the (110) reflection of the β phase at lower temperatures for $D=7.5$ nm, left, and $D=13$ nm, right. The splitting as expected for α-β transition of bulk O_2 is shown for comparison.

In the β phase the linewidth varies from peak to peak in a peculiar way. Here the analysis of the data requires some comments. L is treated as a second-rank tensor, with the major axis along the threefold crystallographic axis. The β structure can be understood as the fcc structure stretched along one of the body diagonals and the axes of the O_2 molecules aligned along this direction. Hence, the β phase is expected to be susceptible to stacking faults and we consider stacking faults as a source of line broadening, in addition to finite size, by generalizing the pertinent models developed for spherical close-packed structures.[23–25] The determination of the width of the peaks (003), (110), (006), and (113) is straightforward, since these peaks do not overlap with others. Furthermore, it turns out that these peaks are not affected by stacking faults. Hence their intrinsic width is related to L. The components of the L tensor, L_c, and $L_\perp (=L_a=L_b)$ can be determined directly from the width of (003) [or (006)] and (110), respectively. The widths of the overlapping peaks (101) and (012), which form the broad maximum around $2\theta=33$ deg, have been derived from fits of a two-peak profile keeping the intensity ratio of the two peaks fixed at the value of bulk β-O_2. The stacking fault probability w is then obtained from the width in excess to what is caused by finite size. The results are shown in Table I. The values of w suggest that stacking faults are definitely a prominent defect of β-O_2 in pores, but on the other hand they are much less abundant than in the truly spherical close-packed hcp phase of pore-condensed N_2 (with $w=0.3$). The fact that the same value of w has been observed for $D=13$ nm and 7 nm could mean that in β-O_2 the stacking faults are not so much needed for a matching of the crystallites to the pore geometry, but are debris left over from the γ-β transition.

TABLE I. Coherence length L of the γ phase, the coherence lengths in the basal plane and along c, $L_\perp$ and L_c, and the stacking fault probability w of the β phase for the three pore diameters D investigated. D and L are in units of nanometer.

	γ phase	β phase		
D	L	$L_\perp$	L_c	w
13	16	12.5	39	0.07
7.5	9	9	23	0.07
5	6	4.5		

Most remarkable are the different values of L_c and $L_\perp$. Whereas $L_\perp$ is of the order of the pore diameter, L_c is about three times larger. Obviously the β crystallites can grow along c over a considerable distance. This must mean that they have a strong tendency of being aligned with the c axis along the pore, which in turn requires the molecular axes to point along c, parallel to the walls. Analogous observations have been made for the hcp phase of pore-condensed N_2 and CO.[8,9]

B. Phase transitions

The freezing and melting of the capillary condensate can be identified through the appearance and disappearance of the Bragg peaks of the γ phase and somewhat more indirectly from the concomitant change of the intensity of the amorphous or fluidlike component of the diffraction pattern. Figure 5 shows the integrated intensity of the $(210)_\gamma$ reflection for $D=7.5$ nm. Freezing starts at 49.2 K and is more or less complete at 48 K. Melting starts at 48 K and is completed at about 52 K. Thus the liquid-solid transformation of the capillary condensate shows a thermal hysteresis, both

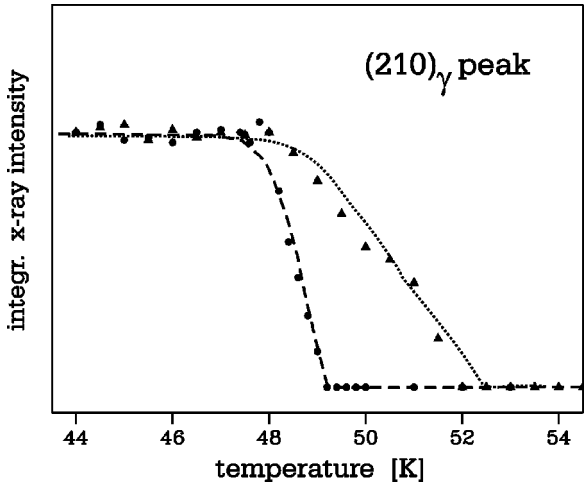

FIG. 5. The variation of the integrated intensity of the (210) peak of the γ-phase upon freezing (●) and melting (▲) for $D=7.5$ nm.

freezing and melting taking place significantly below the bulk triple point T_3, the melting process being smeared out over a larger T range than freezing. These observations are in qualitative agreement with previous work on O_2 (Refs. 2 and 3) and other molecules embedded in nanometer pores. As we have shown recently for the melting of Ar, such a behavior can be explained in terms of a first-order phase transition in a confined cylindrical geometry, an important point being the intrusion of a wetting layer of the high-T phase between the pore wall and the low-T phase in the pore center.[7] For a quantitative comparison with previous results on O_2, we define the freezing and melting temperature T_f and T_m as the midpoints of the liquid-solid coexistence regions on cooling and heating. Figure 6 shows a compilation of all data available from the literature on the freezing and melting points of O_2 in porous glasses. T_3-T_m and T_3-T_f are reasonably well proportional to $1/D$. This kind of dependence has been mentioned in many previous publications on pore melting.[5,6,26–28] The problem is that (i) this relation is of little predictive value since it results quite generally from the competition of a volume-free energy and an interfacial energy and that (ii) it is not clear at all whether this relation is exactly fulfilled or not, mainly because the D values are subject to large systematic errors and because different groups of authors use different ways for the determination of D.

Figures 7–10 illustrate the γ-β transition of pore condensed O_2. Figure 7 shows the T dependence of the intensity of two selected Bragg peaks representing the two phases involved for $D=7.5$ nm and 13 nm. There is considerable thermal hysteresis, even more than for the freezing/melting transition. The width of γ-β coexistence is about 2 K both on cooling and on warming. Figure 6 shows the transformation temperatures $T_{\gamma\text{-}\beta}$ (for cooling) and $T_{\beta\text{-}\gamma}$ (for warming), as determined from the midpoints of the coexistence regions, plotted as function of $1/D$. The data of previous studies is also included. The value of $T_{\gamma\text{-}\beta}=44$ K (and also of $T_f=50$ K) reported by Schirato *et al.* for $D=6$ nm is rather close to the bulk value, which may mean that the diffraction patterns of these authors were actually contaminated by a contribution of bulk material. The transformation temperatures are again roughly proportional to $1/D$. For $D=7.5$ nm and 13 nm, the γ-β transition is more or less complete, even though occasionally we have observed γ residues temperatures well below $T_{\gamma\text{-}\beta}$. See e.g. the weak $(210)_\gamma$ peak in the 25 K pattern of Fig. 2.

For the sample with the smaller pores ($D=5$ nm), however, the γ-β transformation of the capillary condensate is

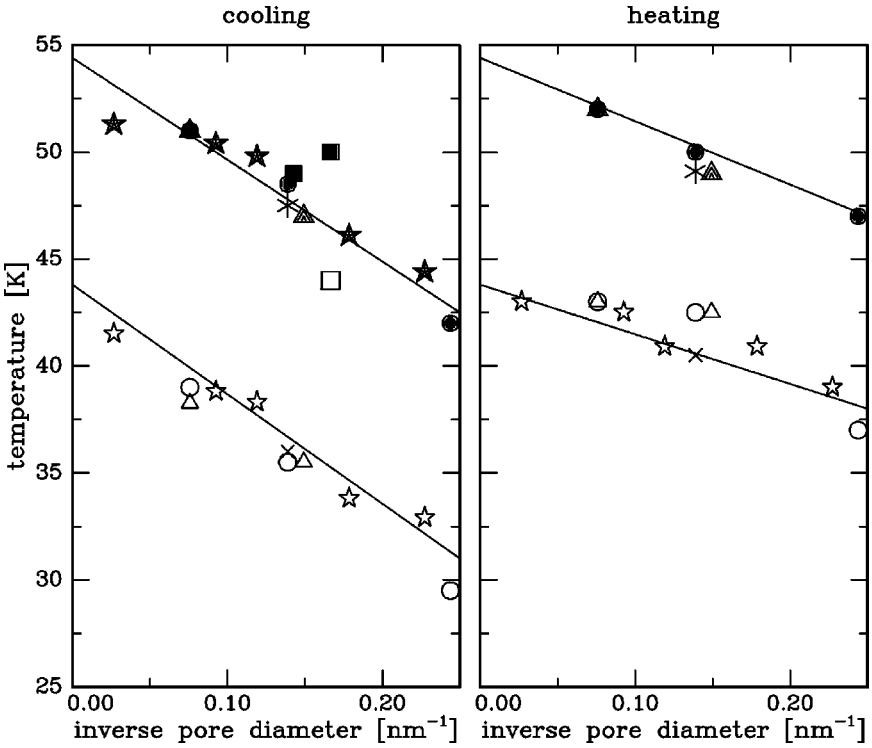

FIG. 6. Phase-transition temperatures of O_2 plotted vs the inverse pore diameter. This study: (●,○), Ref. 15: (■,□), Ref. 22: (▲,△), Ref. 2: ⋆ (filled and empty), Ref. 3: (*,×). The first symbol stands for freezing and melting, the second for the solid-solid transition that in the diffraction studies is identified as γ-β transition.

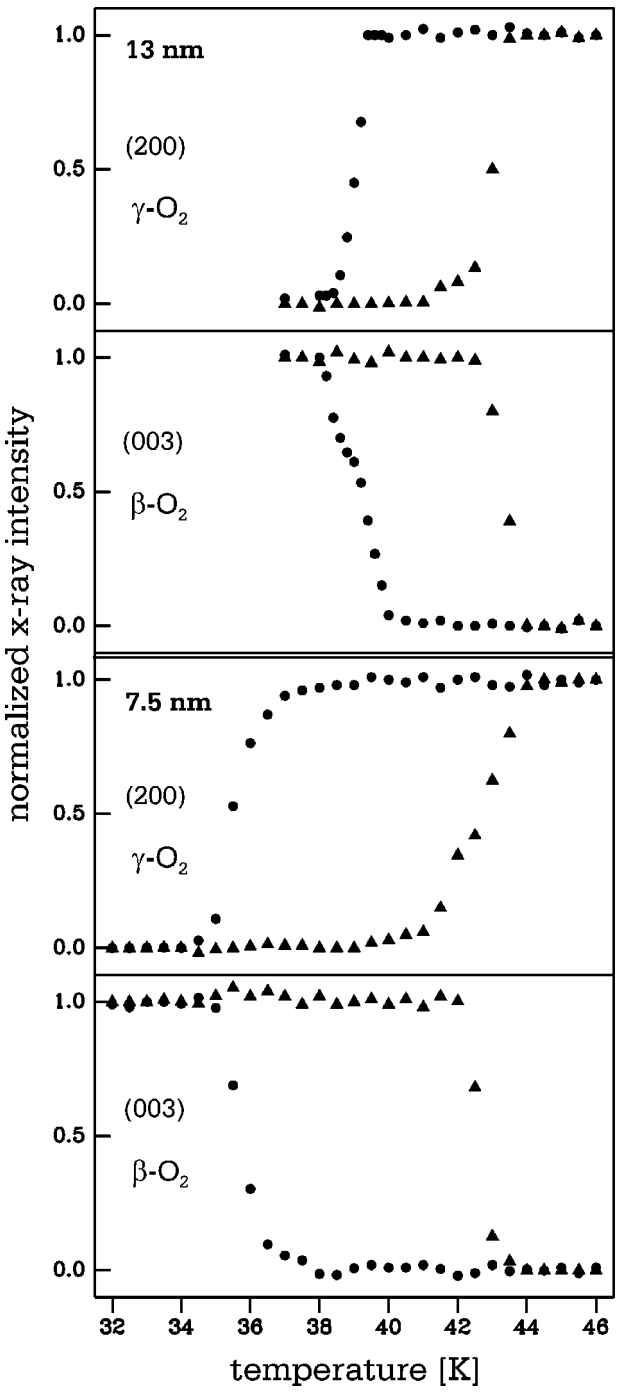

FIG. 7. The variation of the integrated intensity of the (200) reflection of the γ phase and of the (003) reflection of the β phase across the γ-β transition for cooling (●) and heating (▲) for $D=13$ nm and 7.5 nm.

incomplete. This is illustrated in Fig. 8. The diffraction patterns at higher temperatures, e.g., at 36 K for cooling and 41 K on heating are single phase γ. The patterns at low temperatures are superpositions of γ and β patterns, as can be seen, e.g., from the coexistence of $(210)_\gamma$ and $(110)_\beta$. The variation of the volume fractions of the three phases liquid, γ, β with temperature is shown in Fig. 9. The β fraction stabilizes at low T at about 40%.

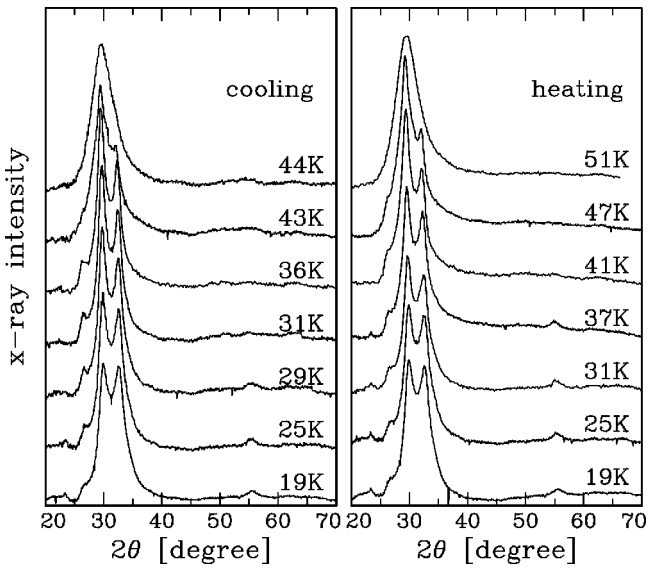

FIG. 8. Diffraction patterns for an almost complete filling ($f=0.90$) for $D=5$ nm. The patterns are actually the differences between $f=0.90$ and $f=0.41$ and, therefore, represent the capillary-condensed part of the pore filling, only.

Figure 10 displays the T dependence of the molar volume v_m as derived from the peak positions of the γ and the β phase. For $D=5$ nm, v_m values for both phases are available over a wide T range because of the incomplete transformation. v_m of the capillary condensate is larger than for the bulk and it increases with decreasing pore size. (For clarity, the values for $D=13$ nm are not included in the figure, they are slightly lower, but very close to the values for 7.5 nm.) The difference between the molar volumes of the β and the γ phase appears to be the same as for bulk O_2. In the β phase the excess of the molar volume with respect to the bulk is practically entirely due to an increased value of the lattice parameter a, rather than c. See the (110) position in Fig. 4. Note that the Bragg angle of this peak depends on a, only. We think that this peculiar increase of the cell volume

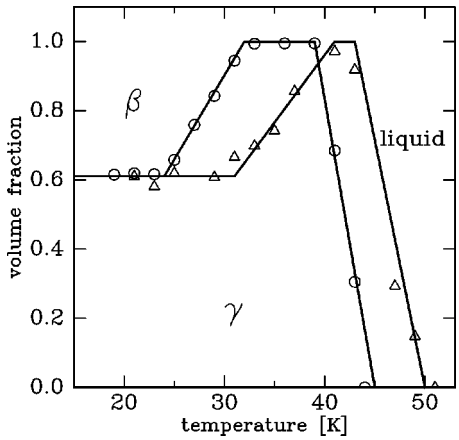

FIG. 9. Volume fraction (as derived from the intensities of the Bragg-reflections of the γ and the β phase) of the phases liquid, γ, β of the capillary condensate in 5-nm pores as function of temperature on cooling (○) and heating (△).

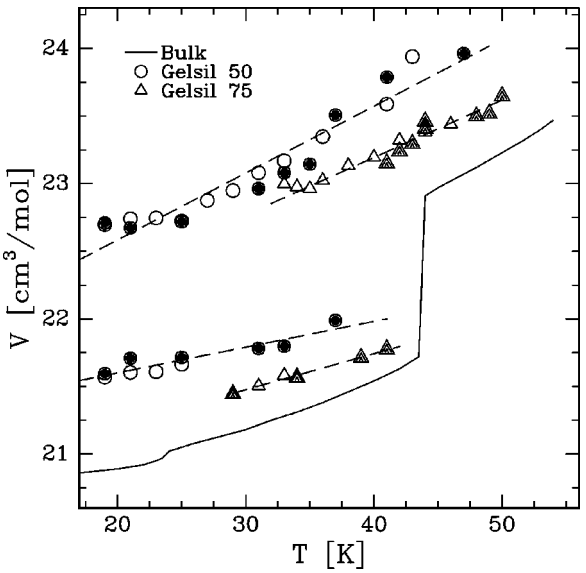

FIG. 10. Temperature dependence of the molar volume of the γ and β phase in pores with $D=5$ nm (●,○) and 7.5 nm (▲,△). Open symbols refer to cooling and closed ones to heating. The solid line is for bulk O_2, Ref. 11.

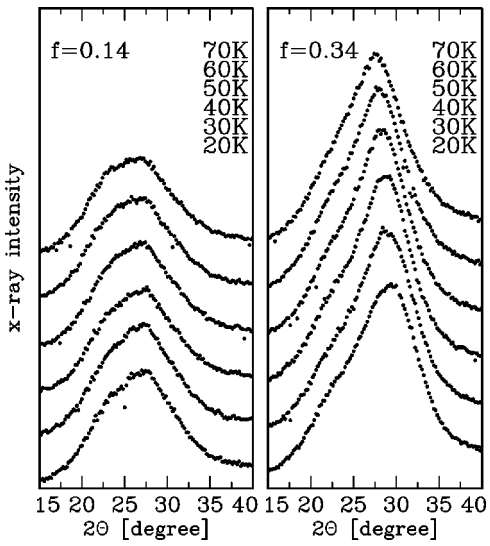

FIG. 11. First maximum of the diffraction pattern of the amorphous component of the pore filling, $D=5$ nm, $f=0.14$ and 0.34, equivalent to about 1 and 2 ML on the pore walls. The background of the substrate has been subtracted.

is due to the lattice defects that are necessary in order to match the crystallites to the pore geometry. The strain field in the vicinity of such a defect also changes the orientations of the neighboring O_2 molecules. In the β phase the molecules next to a defect are tilted out of the c direction, thereby expanding the lattice within the basal plane, but with practically no effect along c.

There is some dependence of the structural properties and of the phase-transition temperatures of the capillary condensate on the fractional filling f for a given porous matrix. Thus the Bragg peaks for low f values slightly larger than f_c are a bit broader than for complete fillings. It is the melting temperature T_m that shows the strongest f dependence. For $D=7.5$ nm, $T_m=47$ K, 48 K, and 50 K and for $f=0.36$, 0.43, 0.89, respectively. Such effects are readily explained by the pore size distribution. The narrower pores are the first to fill on adsorption and to undergo a phase transition on heating.

C. Amorphous component

Figure 11 shows the (first) maximum of the diffraction pattern of the amorphous component ($f=0.14$ and 0.34) in 5-nm pores. For the lower filling, $f=0.14$ that corresponds to somewhat less than 1 ML adsorbed on the pore walls, this feature shows no T dependence. We think that here the O_2 molecules are basically immobile, pinned to favorable adsorption sites on the pore walls. For $f=0.34$, equivalent to roughly 2 ML, there is still no evidence for any major structural change, such as a phase transition, even though the maximum shifts to larger scattering angles and sharpens somewhat on cooling. Obviously the upper part of the adsorbed bilayer does show thermal contraction and some increase of the correlation length towards low T. Note that the overall intensity of the maximum is about T independent. We mention this point explicitly because of an intriguing observation of Schirato *et al.* For a slightly underfilled sample of O_2 in a xerogel with $D=3.5$ nm, these authors have observed a neutron-diffraction pattern that at 60 K is of the same type as those shown in Fig. 11 (and in Fig. 2, $T=50$ K). At 20 K, however, the maximum of the structure factor had almost completely disappeared. Such a change could be due to a distillation of material out of the pores, but they reject this simple explanation and suggest instead that the loss of the maximum is due to an increase in structural disorder, such that at low temperatures the amorphous pore solid is more disordered than the liquid. Our results do not agree with this reasoning.

D. Comments on the γ-β transition

The γ-β transition of pore-condensed O_2 shares many features with pore melting and freezing: The transition temperature is lowered with respect to the bulk state, the temperature shift ΔT being roughly proportional to $1/D$; the transition shows thermal hysteresis and involves phase coexistence; and the heat capacity anomalies have a shape very similar to those of freezing and melting.[3]

The γ-β transition of bulk O_2 is a reconstructive transition, with no group-subgroup relation between the high-T and the low-T phase and hence necessarily of the first order. Reconstructive and other ''martensitic'' transitions[29,30] are known to react sensitively to lattice defects by showing thermal hysteresis and occasionally incomplete transformations. This is so because transformation strains play a vital role. The local strain fields surrounding the defects, subsitutional as well as topological ones, interfere with the transformation strains and thus modify the nucleation and growth of the product phase. Thus there is practically no thermal γ-β hysteresis in well-annealed bulk O_2 samples, but in O_2-rich precipitates from Ar-O_2 mixtures, that is in microcrystals possi-

bly containing a few percent of Ar impurities, a hysteresis of 5 K has been observed.[31] Clearly, there are lots of defects in pores and the effects just described are expected to be important for a detailed understanding of the γ-β transition in narrow pores. On the other hand one would not understand why ΔT should be proportional to $1/D$ in this scenario. This peculiar behavior rather points to a geometric origin. We recall that the simple phenomenological model we have proposed recently for the freezing and melting in pores is by no means specific to a melting transition, but can be applied to the present case as well. For a completely filled pore, there are three relevant interfacial energies, $\sigma_{w\gamma}$, $\sigma_{w\beta}$, and $\sigma_{\gamma\beta}$. The subscripts denote the phases that are in contact at the interface, ''w'' stands for the pore wall or more exactly for the amorphous layer on the walls. In the pores, $T_{\gamma\beta}$ is shifted downward and the γ phase thus stabilized with respect to the β phase. This suggests that $\sigma_{w\gamma}<\sigma_{w\beta}$ which is in agreement with the idea that a disordered phase should be able to adjust more easily to a particular geometry. In fact, orientationally disordered ''plastic'' phases are known to have very low surface energies with respect to the liquid and often do not show any faceting. Let us, therefore, assume that $\Delta\sigma=\sigma_{w\beta}-\sigma_{w\gamma}-\sigma_{\gamma\beta}>0$. In case this relation holds, the γ-β transition can proceed as follows: Already at low temperatures, well below $T_{\gamma\beta}^{\mathrm{bulk}}$, a cylindrical shell of the γ phase intrudes between the amorphous layer on the pore walls and the γ phase in the pore center, thereby reducing the interfacial energies at the expense of volume-free energy. On warming, the thickness of this shell increases and finally at a characteristic temperature T_0, $T_0<T_{\gamma\beta}^{\mathrm{bulk}}$, the remaining β solid transforms all at once into γ. This happens when the release of interfacial energy to the elimination of the γ-β interface is equal to the latent heat necessary for the γ-β transition of the core. The model ignores any pressure difference across the curved interface and thus implicitly assumes that the phases are incompressible. It supplies a natural explanation of the $1/D$ dependence and the thermal hysteresis of $T_{\gamma\beta}$. See Ref. 7 for the free-energy functional, metastable states, and an example of the T dependence of the fraction of the high-T phase.

The results of the present experiments are in general agreement with this view but on the other hand cannot produce direct proof for the model. The low-T γ fraction for $D=5$ nm and even the low-T γ remainders in the larger pores mentioned earlier should not be identified with what is called above an intruding γ shell. Varying $\Delta\sigma$ within reasonable limits suggests that this shell should never grow larger than 1 or 2 ML and it is obvious that the diffraction pattern of such a thin layer would be very weak and would have no more than little resemblance with the pattern of bulk γ. Thus, it is presumably more appropriate to refer not to a layer of γ material but to a ''matching'' layer that mediates between the β solid in the pore center (with molecules oriented preferentially along the pore axis) and the amorphous bilayer on the pore walls (perhaps with molecules preferentially aligned perpendicular to the walls).

A complete understanding of the γ-β transition also has to consider network effects. Here concepts developed for pore filling and emptying in context with sorption isotherms may be helpful.[32] The change of the γ-β interface with T is in fact analogous to that of the vapor-liquid interface as function of vapor pressure. The γ-β transition at T_0 in the former case corresponds to capillary condensation in the latter. The propagation of the γ-β interface through the pore network due to nucleation and growth is likely to be a percolation-type process that depends sensitively on the connectedness and the accessibility of the cavities and throats of the pore network. Such effects should be more pronounced the smaller the pore diameter and perhaps lead to the incomplete transformation in the 5-nm pores.

IV. SUMMARY

Obviously solid O_2 in pores down to at least 5 nm forms a nanocrystalline component in addition to an amorphous component next to the walls. The nanocrystalline component obeys the phase sequence liquid-γ-β of the bulk system. We find the formation of a crystalline solid, of the γ solid in particular, in pores as narrow as 5 nm quite remarkable. After all, the pore diameter available for the capillary condensate amounts to just a few lattice parameters, 6 in fact for the γ solid in the 5-nm pores. Furthermore, the building principle of the γ phase, a stacking of ''spheres'' and ''disks,'' is definitely much more intricate than the simple close packing of spheres of, e.g., fcc Ar or hcp β-N_2 and CO.

In order to match to the walls, the nanocrystalline solid has to pay a price in the form of lattice faults; one type of which, namely, stacking faults of β-O_2, could be identified in the diffraction pattern. The size of the crystallites in the radial direction is limited by the pore walls. Along the pore axis the crystalline coherence can extend over somewhat larger distances. In the β phase the main symmetry axis of the lattice and the molecular axes show a preference of being aligned parallel to the pore axis.

The question whether the α-β transition takes place in the pores could not be definitely answered. Presumably there is still an antiferromagnetic ordering of the spins, but the magnetoelastic deformation is reduced. Melting and freezing appear to be analogous to pore-condensed Ar. The γ-β transition is particularly sensitive to the confinement in the pores. In the smallest pores studied this transformation remains incomplete. The peculiar behavior of both the melting and the γ-β transition with a $1/D$ dependence of the downward shift of the transition temperature, thermal hysteresis with respect to cooling and heating and coexistence regions appears to be a natural consequence of the confined geometry: the high-temperatures phase nucleates first as thin layer next to the pore walls and finally spreads across the pores, a process similar to capillary condensation.

Note added in proof. Recently, another article on oxygen in mesopores has been published.[33]

ACKNOWLEDGMENT

This work has been supported by the Sonderforschungsbereich 277.

[1] J.L. Tell and H.J. Maris, Phys. Rev. B **28**, 5122 (1983).
[2] D.D. Awschalom and J. Warnock, Phys. Rev. B **35**, 6779 (1987).
[3] E. Molz, A.P.Y. Wong, M.H.W. Chan, and J.R. Beamish, Phys. Rev. B **48**, 5741 (1993).
[4] E.B. Molz and J.R. Beamish, J. Low Temp. Phys. **101**, 1055 (1995).
[5] K. Morishige and K. Kawano, J. Chem. Phys. **110**, 4867 (1999).
[6] R. Radhakrishnan, L. Gelb, and E. Gubbins, Langmuir **15**, 6060 (1999).
[7] D. Wallacher and K. Knorr, Phys. Rev. B **63**, 104202 (2001).
[8] P. Huber, D. Wallacher, and K. Knorr, J. Low Temp. Phys. **111**, 419 (1998).
[9] P. Huber, D. Wallacher, and K. Knorr, Phys. Rev. B **60**, 12 666 (1999).
[10] G.C. DeFotis, Phys. Rev. B **23**, 4714 (1981).
[11] I.N. Krupskii, A.I. Prokhvalitov, Y.A. Freiman, and A.I. Erenburg, Fiz. Nizk. Temp. **5**, 271 (1979) [Sov. J. Low Temp. Phys. **5**, 130 (1979)].
[12] C.S. Barret, L. Meyer, and J. Wasserman, Phys. Rev. **163**, 851 (1967).
[13] S. Gregory, Phys. Rev. Lett. **39**, 1035 (1977).
[14] S. Gregory, Phys. Rev. B **23**, 415 (1981).
[15] B.S. Schirato, M.P. Fang, P.E. Sokol, and S. Komarneni, Science **267**, 369 (1995).
[16] P. Levitz, G. Ehret, S.K. Sinha, and J.M. Drake, J. Chem. Phys. **95**, 6151 (1991).
[17] A.Ch. Mitropoulos, J.M. Haynes, R.M. Richardson, and N.K. Kanellopoulos, Phys. Rev. B **52**, 10 035 (1995).
[18] Lev D. Gelb and K.E. Gubbins, Langmuir **14**, 2097 (1998).
[19] S. Brunauer, P.H. Emmett, and E. Teller, J. Am. Chem. Soc. **60**, 309 (1938).
[20] W.F. Saam and M.W. Cole, Phys. Rev. B **11**, 1086 (1975).
[21] P. Huber and K. Knorr, Phys. Rev. B **60**, 12657 (1999).
[22] R. Ackermann, T. Knoblauch, D. Kumar, K. Unger, and M. Enderle, J. Low Temp. Phys. **122**, 143 (2001).
[23] A. Gunier, in *X-Ray Diffraction in Crystals, Imperfect Crystals and Amorphous Bodies* (Dover, New York, 1994), p. 219.
[24] H. Jagodzinski, Acta Crystallogr. **2**, 201 (1949).
[25] B. E. Warren, *X-Ray Diffraction* (Addison-Wesley, Reading, MA, 1969).
[26] K.M. Unruh, T.E. Huber, and C.A. Huber, Phys. Rev. B **48**, 9021 (1993).
[27] C.L. Jackson and G.B. McKenna, J. Chem. Phys. **93**, 9002 (1990).
[28] R. Mu and V.M. Malhotra, Phys. Rev. B **44**, 4296 (1991).
[29] P. Tolédano and V. Dmitriev, *Reconstructive Phase Transitions* (World Scientific, Singapore, 1996).
[30] Z. Nishiyama, *Martensitic Transformation* (Academic Press, New York, 1978).
[31] J. Xie, M. Enderle, K. Knorr, and H.J. Jodl, Phys. Rev. B **55**, 8194 (1997).
[32] Y. C. Yortsos, in *Methods in the Physics of Porous Media*, edited by Po-Zen Wong (Academic Press, San Diego, 1999), p. 69.
[33] K. Morishige and Y. Ogisu, J. Chem. Phys. **114**, 7166 (2001).